Lab on a Chip

Functional Screening of Antibody-Secreting Cells by Co-Culture with Reporter T Cells Using PicoShells

Journal:	*Lab on a Chip*
Manuscript ID	LC-ART-04-2025-000319.R2
Article Type:	Paper
Date Submitted by the Author:	11-Jun-2025

Complete List of Authors:	Nishimoto, Kazuki; The University of Tokyo, Mechano-Informatics; University of California Los Angeles, Bioengineering Ghosh, Rajesh; University of California Los Angeles, Bioengineering van Zee, Mark; University of California Los Angeles, Department of Bioengineering Fang, Darren; University of California Los Angeles, Bioengineering Mao, Zhiyuan; University of California Los Angeles, Molecular and Medical Pharmacology Noguchi, Miyako; University of California Los Angeles, Molecular and Medical Pharmacology Di Carlo, Dino; University of California Los Angeles, Bioengineering; CNSI; University of California Los Angeles, Mechanical Engineering; University of California Los Angeles Jonsson Comprehensive Cancer Center

Functional Screening of Antibody-Secreting Cells by Co-Culture with Reporter T Cells Using PicoShells

Kazuki Nishimoto[1,2], Rajesh Ghosh[2], Mark van Zee[2], Darren Fang[2], Zhiyuan Mao[3], Miyako Noguchi[3], Dino Di Carlo[2,4,5,6].

[1]Department of Mechano-Infomatics, Graduate School of Information Science and Technology, The University of Tokyo, Bunkyo, Tokyo, 113-8656 Japan.

[2]Bioengineering department, University of California, Los Angeles, CA 90095 USA.

[3]Department of Molecular and Medical Pharmacology, David Geffen School of Medicine, University of California, Los Angeles, CA 90095 USA.

[4]California NanoSystems Institute (CNSI), University of California, Los Angeles, CA 90095 USA.

[5]Department of Mechanical Engineering, University of California, Los Angeles, CA 90095 USA.

[6]Jonsson Comprehensive Cancer Center, University of California, Los Angeles, Los Angeles, CA 90095, USA.

Abstract

Monoclonal antibodies (mAbs) are a growing class of therapeutics known for their high specificity and diverse functional mechanisms, including agonism and antagonism. Although microwell array technologies and droplet microfluidics are employed to pair antibody-secreting cells (ASCs) with target cells for therapeutic mAb discovery, existing methods suffer from limited throughput or inadequate functional assessment. To address these limitations, we applied PicoShells, hollow media-permeable hydrogel microparticles, to evaluate mAb function by co-culturing assay of hybridomas with reporter cells for 24 hours. Using this workflow, we identified hybridomas secreting antibodies that modulate the expression of nuclear factor of activated T cells (NFAT) in co-encapsulated reporter cells. High-throughput fluorescence activated cell sorting (FACS) of PicoShells containing cells from a spiked population identified active clones, which were sorted, expanded, and validated post-selection, demonstrating 79.4% T cell activation, a 5.2-fold enrichment in functional clones over the starting spiked population. This approach integrates functional assessment with scalable processing, offering a robust solution for screening antibody libraries and accelerating therapeutic discovery.

Introduction

Antibody therapeutics have transformed modern medicine, with over 100 mAbs, produced by ASCs, approved worldwide[1]. Traditional methods for developing effective mAbs focus on identifying binders based on affinity to a target (e.g. using phage/yeast display or antigen baiting of memory B cells), followed by labor-intensive functional testing using cellular reporter assays to identify leads with desired activities, such as pathway activation or cell growth stimulation[2]. The effectiveness of antibodies relies on the ability to not only bind to specific molecular targets, but also elicit functional cellular responses, modifying intracellular gene expression through agonism or antagonism[3]. Especially in T cells, antibodies can regulate complex signal transduction pathways[4–6], neutralize soluble cytokine signaling molecules, and recruit immune effector functions upon binding—all crucial factors that influence therapeutic efficacy. Performing affinity assays and functional screening separately leads to costly re-expression of many

candidates and can miss rare antibodies with critical therapeutic effects. To address these challenges, numerous efforts are currently focused on developing high-throughput, function-first strategies that assess ASCs for their effects on target cells.

Compartmentalized co-culture systems, which pair single ASCs with target reporter cells, provide an approach for assessing antibody function. Existing microwell formats can achieve pairing but lack the scalability needed to assess larger libraries of ASCs comprehensively[7,8]. Conventional systems like the Beacon® Optofluidic System (Bruker, Billerica, MA, USA) have limitations for high-throughput co-culture, including non-standard culture conditions, limited scalability (~10,000 cells), high cost, and dependence on proprietary reagents and training[9]. Droplet microfluidics, widely used in single-cell high-throughput screening and sequencing workflows, have been used for functional antibody screening[10–13]. However, the platform faces challenges that limit the timeframe to study antibody effects, due to the limited stability and suboptimal gas and nutrient exchange in water-in-oil emulsions[14,15], making it challenging to evaluate functional cellular responses or cell–cell interactions mediated by secreted antibodies. Additionally, conventional droplet systems require specialized, often unavailable custom sorters, which increase the risk of droplet coalescence or rupture and thus limit sorting rates to prevent breakage[14,16,17]. Although researchers have applied hydrogel microparticles to encapsulate single ASCs enabling high-throughput screening on standard flow sorters, target-expressing cells that can report on the function of the secreted antibodies were not co-encapsulated[18,19]. These previous works evaluated antibody affinity and binding, rather than directly assessing functional signaling in target cells.

To overcome the limitations of existing functional screening platforms, we employed PicoShells—polyethylene glycol (PEG)-based core–shell hydrogel microparticles[20]—as a scalable system for antibody screening (Figure 1). These picoliter-sized hollow compartments allow nutrient transport, support microscale co-culture, and are compatible with standard fluorescence-activated cell sorting (FACS). While PicoShells have previously been used for selecting fast-growing or high metabolite-producing algae or yeast cells, their application to functional assays involving cell–cell interactions have not been explored. To enable such assays, we first characterized key parameters—co-encapsulation efficiency, cell viability, and potential antibody transport across the hydrogel matrix—to ensure reliable co-culture conditions and functional antibody detection.

As a model ASC, we used OKT3 hybridomas, which secrete the widely used anti-CD3 monoclonal antibody[21]. OKT3 and NFAT-reporter T cells were co-encapsulated in hydrogel shells, where secreted functional antibodies activated TCR signaling, inducing GFP expression in T cells. We first confirmed efficient co-encapsulation and high post-fabrication viability. GFP signals were detected only when functional hybridomas were present, validating assay specificity. Using a 1:10 mixture of functional to non-secreting cells, we demonstrated successful enrichment of antibody-secreting clones. Finally, we confirmed that sorted hybridomas remained viable and expandable. Together, this PicoShell-based approach provides a robust, high-throughput platform for highly functional screening of antibody-secreting cells based on biologically meaningful interactions—offering a streamlined strategy to isolate rare, high-potency clones even from monoclonal populations.

Experimental Section

Cell Line and Culture

OKT3 cells were acquired from the American Type Culture Collection (ATCC, Manassas, VA, USA). HyHEL5 cells were provided by Richard Willson from the University of Houston Department of Biology and Biochemistry. MF20 was purchased from the Developmental Studies Hybridoma Bank (DSHB; Iowa City, IA, USA). Reporter Jurkat cells, namely Jurkat-NFAT-GFP and Jurkat-NFAT-GFP-F5 TCR, were obtained from the Witte lab at University of California, Los Angeles[22]. All hybridomas were cultured in Iscove's Modified Dulbecco's Medium (IMDM; Gibco, Grand Island, NY, USA), while Jurkat cells were maintained in Roswell Park Memorial Institute Medium (RPMI; Gibco). All culture media were supplemented with 10% non–heat-inactivated fetal bovine serum (FBS; Gibco, Grand Island, NY, USA) and 1% antibiotics-antimycotics (Gibco, Grand Island, NY, USA). During the culture, the cells were incubated at 37 °C in a humidified atmosphere containing 5% CO_2.

Reporter Cell Line (Jurkat-NFAT-GFP-TCR), CD3 expression level assay

The Jurkat-NFAT-GFP-TCR line was engineered from CD3-expressing reporter Jurkat cells by introducing a plasmid encoding GFP under the control of the NFAT promoter. Upon engagement of the T cell receptor (TCR) with functional anti-CD3 antibodies, the cells express GFP (Figure S1, 2).

PicoShell Fabrication

Microfluidic devices were fabricated from polydimethylsiloxane (PDMS; Dow, Torrance, CA, USA) using standard soft lithography techniques. To prevent nonspecific adsorption to channel surfaces, devices were treated with 1% trichloro(1H,1H,2H,2H-perfluorooctyl)silane (Millipore Sigma, Burlington, MA, USA) dissolved in Novec™ 7500 (3M, Maplewood, MN, USA). The PicoShell encapsulation system comprised four input phases: (i) an aqueous cell suspension phase, containing 9.0 mM 40 kDa dextran derived from Leuconostoc spp. (Millipore Sigma, Burlington, MA, USA); (ii) a hydrogel precursor phase, containing 19.1 μM 10 kDa 4-arm polyethylene glycol-maleimide (PEG-Mal; Laysan Bio, Arab, AL, USA); (iii) a cross-linker phase, containing 50 mM dithiothreitol (DTT; Millipore Sigma, Burlington, MA, USA); and (iv) an oil phase, composed of 0.4% (v/v) Pico-Surf surfactant (Sphere Fluidics, Cambridge, UK) in Novec™ 7500.

All aqueous reagents (dextran, PEG-Mal, and DTT) were prepared in phosphate-buffered saline (PBS; pH 6.4, Gibco, Grand Island, NY, USA) supplemented with 5.0 mg/mL glucose (Millipore Sigma, Burlington, MA, USA). Encapsulation was performed using flow rates of 1.2 μL/min (aqueous dextran phase), 0.6 μL/min (PEG-Mal phase), 0.6 μL/min (DTT phase), and 15 μL/min (oil phase). All fabrication and encapsulation procedures were completed within maximum 1.5 hours following initial mixing of the cells with the dextran solution.

Droplet De-emulsification and PicoShell-Cell Culture

Following successful fabrication and particle formation within individual droplets, PicoShells were de-emulsified using 20% (v/v) Pico-Break (Sphere Fluidics, Cambridge, UK), a biocompatible demulsifier, in a Novec™ 7500. Afterward, the PicoShells were collected through a 100 μm cell strainer (Corning, Corning, NY, USA) and resuspended in fresh culture media at 37 °C with 5% CO_2. After about 2 or 3 weeks of culture, the PicoShells burst, allowing for recovery and further culture of hybridoma cells. PicoShell formation is done at room temperature and polymerization is complete once the particles exit the device without any additional incubation.

Flow Cytometry

Single-particle fluorescence analysis was conducted using an SH800 Cell Sorter (Sony, Tokyo, Japan). Droplet throughput was first calibrated to 2000 events per second, and during measurements, samples were diluted with PBS to maintain event rates between 100 and 800 events per second. For PicoShell sorting, we adjusted the event rate to ~150 Hz, ensuring single-PicoShell sorting. Flow cytometry data were analyzed using the fluorescence Area or Height intensity, which represents the integrated signal across the duration of each event, or the maximum fluorescence peak Height.

Functional Assay

Functional validation of OKT3 was achieved through co-culturing with reporter T cells stained with 1 μM CellTracker Deep Red and hybridoma cells stained with 200 μM CellTracker Blue. Initially, 2.0 x 10^5 reporter T cells and 1.0 x 10^5 hybridoma cells were mixed, maintaining an equal cell count for each cell type. After 24 hours of co-culture, flow cytometry was performed to determine the GFP-positive ratio among Cy5-positive reporter cells, providing a measure of OKT3 functionality. Each dot in the figure represents a technical replicate from the same sample, measured independently to confirm consistency.

Results and Discussion

Hybridoma and reporter T cell co-encapsulation within PicoShells

We co-encapsulated OKT3 with engineered reporter T cells during PicoShell fabrication using a microfluidic droplet generator (Figure 1B, C, Figure S3A-B). Cells suspended in a dextran solution were co-flowed with 4-arm PEG-maleimide and dithiothreitol (DTT) solutions before droplet generation, allowing the PEG-maleimide to phase separate and crosslink into an outer hydrogel shell (Figure S3C-E) with exposure to DTT. Dextran phase separates to the core remaining uncrosslinked and later diffuses outside of the PicoShells. The cells remain encapsulated within the hollow cavity of the PicoShells, which did not contain any polymerized PEG material (Movie S1, S2). With a fabrication rate of ~2 kHz, we produced ~7.2 million PicoShells per hour. Additional PicoShells can be continuously produced by exchanging the dextran/cell mixture periodically to expand screening capacity. The fabricated PicoShells had a uniform diameter of 49.5 μm with a coefficient of variation (CV) of 6.8% (n = 2467) (Figure S3F). We quantified the number of hybridoma and reporter T cells encapsulated within individual PicoShells at a 1:2 ratio (Figure 2, n = 2371; Table S1). The analysis revealed that 4.6% of PicoShells encapsulated hybridomas, 18.2% contained reporter T cells, and 2.1% co-encapsulated both cell types, resulting in an estimated double encapsulation of approximately 144,000 PicoShells containing both hybridomas and reporter T cells within one hour of encapsulation, enabling sufficient throughput for large-scale screening. Further improvements in double encapsulation frequency may be achievable using microfluidic designs that order cells prior to encapsulation[23–26], because the encapsulation ratio follows a Poisson distribution. This distribution can occasionally result in undesired combinations, such as co-encapsulation of target, off-target, and reporter cells, producing GFP signals associated with a mixed population of ASCs. Following encapsulation, the PicoShells were removed from the emulsions and incubated in suitable media.

To assess whether the fabrication process affects cell viability, we performed a live/dead assay on hybridoma cells before and after encapsulation in PicoShells (Figure S4). Prior to encapsulation, cell viability was 98.6%. Immediately after encapsulation, viability was 98.4%. These results indicate that the fabrication process—including exposure to surfactants and DTT—does not significantly compromise cell

viability. The use of biocompatible reagents such as PicoSurf® and PicoBreak™, along with the rapid maleimide-thiol crosslinking reaction and moderate pH, helps preserve cell health during encapsulation[20]. In addition, nutrients can freely diffuse into the PicoShells, supporting continued cell viability as cells grow over multiple days (Figure S4 and Figure S5). After three days of culture, viability was 97.4%. The apparent increase in viability may be attributed to challenges in quantifying overlapping cells appearing as double-positive in 2D fluorescence images due to stacking within the hollow hydrogel structure (Figure S4B). We also evaluated T cell proliferation within PicoShells over a 3-day culture period (Figure S5). These data confirm that both hybridoma and T cells remain viable and capable of growth for several days within the PicoShells.

T cell activation with antibody secreted from OKT3 hybridoma in PicoShells

After a day of co-culture, co-encapsulated OKT3 and reporter T cells were analyzed by FACS to assess whether the secreted mAbs could bind and cluster CD3/TCRs, thereby triggering NFAT activation. PicoShells containing cells showed higher forward scatter (FSC) and side scatter (SSC) values than empty PicoShells which had lower FSC and SSC values (Figure 3A). Within these high FSC/SSC events, gated as "cell-containing PicoShells" in Figure 3A (upper gate), were further segmented based on CellTracker Blue and CellTracker Deep Red fluorescence, which respectively labeled hybridoma and T cells. The population located between the empty and cell-containing PicoShell clusters on the scatter plot likely represents free, non-encapsulated cells that were never encapsulated or were released from PicoShells.

Three PicoShell sub-populations were observed: CellTracker Blue-negative/CellTracker Deep Red-positive (reporter T cells only), blue-positive/deep red-negative (OKT3 hybridomas only), and double-positive (both cell types), together accounting for 6.68% of the cell-containing events (Figure 3B). Microscopy of sorted PicoShells confirmed the presence of cells in each sub-population. The GFP positivity threshold was determined based on the distribution of GFP area signal in T cells identified under the blue-negative/deep red-positive population. While only 1–2% of PicoShells containing either hybridomas or T cells alone were GFP-positive, approximately 34% of the double-positive PicoShells (labeled with CellTracker Blue and Deep Red) showed GFP expression (Figure 3C). While this may in part reflect biological heterogeneity among the OKT3 clones, including differences in antibody secretion kinetics or levels, technical factors also contribute to this detection rate. For example, OKT3 functionality may be masked due to false negatives from slow antibody kinetics, or variability in reporter cell responsiveness. In addition, flow cytometry may not reliably detect low or borderline GFP signals, which are determined based on predefined GFP intensity thresholds. Taken together, the observed detection rate likely underestimates the true frequency of functional clones; nevertheless, the platform's high-throughput screening capability combined with functional evaluation of antibody-secreting cells offers valuable potential for use in antibody discovery and development pipelines.

To evaluate antibody containment, we incubated encapsulated or free reporter T cells with OKT3 hybridomas. After 24 hours, encapsulated T cells co-cultured with free OKT3 showed no GFP expression, whereas free T cells displayed elevated GFP (Figure S6A-B). However, T cells within PicoShells could still be activated by phorbol-12-myristate-13-acetate (PMA), a small-molecule protein kinase C (PKC) activator, confirming reporter T cells functionality under the 24-hour assay conditions (Figure S6C). These results demonstrate selective T cell activation by anti-CD3 antibodies secreted from co-encapsulated OKT3 hybridomas, with minimal antibody crosstalk to other PicoShells in the same media environment.

Spiked population screening using HyHEL5 as off-target hybridoma

Functional OKT3 clones were recovered by selecting PicoShell events based on reporter T cell activation from a mixed hybridoma population. We constructed a mixed library (1:10) of on-target and off-target hybridoma including OKT3 clones secreting anti-CD3-specific mAbs and HyHEL5 clones producing HEL-specific mAbs, which do not activate reporter T cells (Figure 4A). The mixed population was co-encapsulated with reporter T cells in PicoShells, cultured for 24 hours, and analyzed via flow cytometry to measure GFP expression as a marker of T cell activation. Populations were gated by GFP intensity (Figure 4B), allowing us to distinguish pre-stained OKT3 or HyHEL5 fractions within each gate (Figure 4C). At a GFP signal threshold of 10^5, the fraction of OKT3 clones increased from the initial 1:10 ratio to 82.1%, saturating at ~95% for the most stringent GFP gates. Higher GFP levels were strongly linked to OKT3 cells, confirming that GFP expression was specifically driven by OKT3 antibodies and not non-specific activation due to co-culture with hybridomas. These results demonstrate that GFP-based T cell activation reliably differentiates on-target hybridomas (such as OKT3) from non-functional ones (such as HyHEL5), validating the assay for high-throughput screening of functional antibody-secreting hybridoma.

Functional evaluation after Picoshell screening of a spiked hybridoma population

Building on the successful identification of functional hybridoma from an initial spiked population, we screened an unstained mixed population containing 10% OKT3 hybridomas, sorted GFP-positive events, regrew clones, and tested mAb function from hybridoma culture supernatant. This experiment simulates library screening, using reporter T cells activation as an indicator of functional antibody activity to identify and select antibody-secreting clones for monoclonal antibody development. To validate and expand the top-performing clones for downstream applications, we conducted an off-chip T cell activation assay to evaluate the functional capacity of enriched clones in a format that closely reflects their intended use.

To assess functional activity, we co-cultured cells for rapid 24 hours, sorted PicoShells with the highest GFP levels, and expanded them in 96-well plates (Figure 5A, B). Over two weeks for the subsequent long-term off-chip expansion of selected clones, selected hybridoma clones expanded to stretch the PicoShells to an average diameter of about 290 μm before bursting the PicoShells and expanding throughout the wells (Figure 5C). To evaluate the functionality of the expanded clones under off-chip conditions, we compared T cell activation in the recovered clone to both the initial 10% OKT3-spiked and 100% OKT3 controls. The recovered clone exhibited a 5.2-fold increase over the starting population and even an 11% increase in functional improvement over the 100% OKT3 group (Figure 5D), which may indicate loss of secretory capacity in a fraction of clones from the initial OKT3 pool. Our results demonstrate that hybridoma clones with enhanced functional activity, as indicated by T cell activation, can be efficiently sorted within PicoShells at high throughputs (~ 540,000 events per hour) and subsequently recovered for downstream validation and selected clone expansion. Although cell expansion can be prolonged and limited by stress or hypoxia, hydrogel degradation post-sort can release cells immediately for oxygen-sensitive applications[20]. Notably, the activation level of the selected hybridoma populations in our screens was higher than that of an unselected OKT3-only population, suggesting the potential to isolate functionally superior antibody-secreting clones even within a monoclonal population. This underscores the potential of high-throughput screening to identify hybridoma clones that both functionally respond to target cells and produce high antibody titers, and the platform may also be applied to screen for ASCs derived from differentiated memory B cells[27].

Conclusions

In conclusion, we developed a high-throughput, functional antibody screening method using PicoShells that leverages microfluidic co-encapsulation, co-culture within selectively permeable core-shell microparticles over >24 hours and is compatible with standard cell sorters for accessible sorting. Our microfluidic droplet generator produced PicoShells at rates of 2 kHz co-encapsulating OKT3 hybridomas and reporter T cells, enabling extended culture (Figure 2). After a day culture, reporter T cell encapsulated with OKT3 was activated and expressed GFP in a PicoShell for a day culture with minimal crosstalk between PicoShells (Figure 3). When off-target HyHEL5 clones were spiked at a 1:10 ratio, GFP-based T cell activation selectively enriched OKT3 to over 80% (Figure 4). Further screening of unstained spiked populations isolated and expanded the functional populations, exhibiting 5.2-fold higher activation levels from supernatants compared with the initial 10% spiked on-target ASCs library, highlighting this approach for large-scale antibody discovery (Figure 5). Once encapsulated, cells can be cultured for several days to promote mAb accumulation from antibody-secreting cells and robust gene activation in target cells. Unlike typical droplet-based systems, PicoShells do not require water-in-oil specific FACS, enabling the isolation of high-performing clones—including rare single-cell hybridomas—that exhibit superior functional activity upon expansion. While several commercial platforms exist for functional screening in semi-confined volumes, such as the Beacon® Optofluidic System (Bruker, Billerica, MA, USA), these systems often require specialized instrumentation, user training, and proprietary reagents, and typically operate under non-standard culture conditions. In contrast, our PicoShell-based platform functions with standard incubators and media, is readily scalable by increasing the number of fabrication runs to match target library sizes, and integrates with conventional FACS workflows using fluorescence-based assays—providing a more accessible and flexible solution for high-throughput co-culture screening. Additionally, while microfluidic expertise is required to generate cell-loaded PicoShells—unlike Nanovial-based approaches[28–30]— the fully encapsulated cells in PicoShells might enable higher mAb accumulation than porous hydrogels particles like agarose, or Nanovials. Despite these limitations, the system provides unique advantages as a robust platform for high-throughput functional screening, with long-term culture and assay (>24 hours) capabilities and selective accumulation of secreted proteins. More broadly, PicoShell co-encapsulation not only enables high-throughput functional screening of mAbs but also provides a platform to model and analyze cell-cell interactions within a controlled microenvironment, potentially enabling additional screens based on functional single-cell assays, like cell killing, cell growth, or gene expression modulation in the future. The throughput of the assay can ultimately drive an exponential increase in data generation from large scale pooled screens, such as genetic perturbation screens.

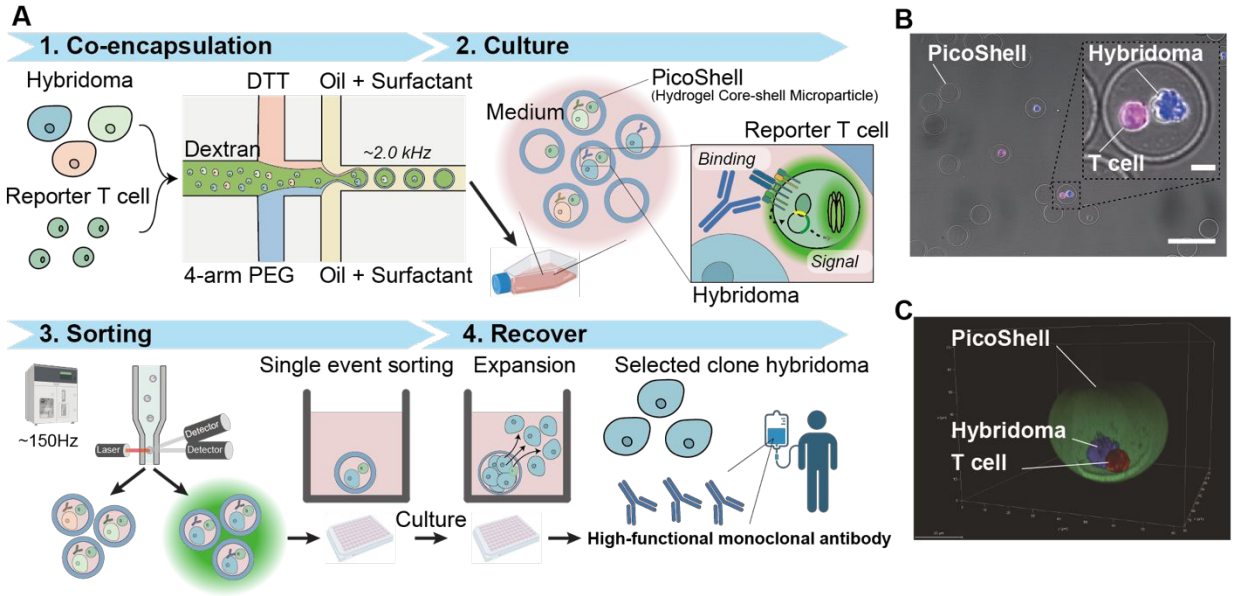

Figure 1. Overview of the PicoShell co-culture screening workflow. (A) Schematic of the PicoShell workflow for functional screening via co-culture of multiple cell types by co-encapsulation. Hybridomas and reporter T cells were co-encapsulated within PicoShells, where reporter T cells were activated by antibodies secreted by the hybridoma. GFP-positive PicoShells were sorted, reflecting T cell activation. Hybridoma clones were recovered by continuous culturing of PicoShells until cell expansion. (B) Fluorescent image of PicoShells with stained Hybridoma (blue, CellTracker Blue) and T cells (magenta, CellTracker Deep Red). Scale bar = 100 µm and 10 µm (insets). (C) Confocal image of a PicoShell (green) encapsulating hybridoma (blue) and T cells (magenta). The scale is indicated in the image.

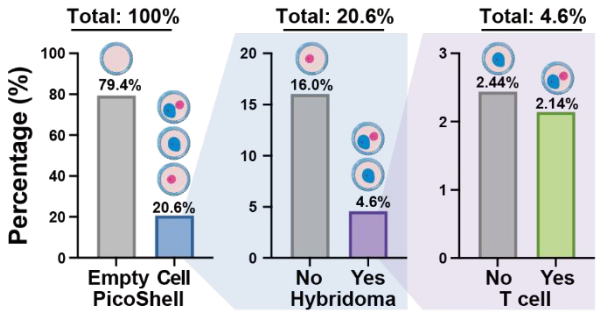

Figure 2. Nested distribution of hybridoma and reporter Jurkat T cells in PicoShells as measured through fluorescence microscopy for PicoShells (n = 2371).

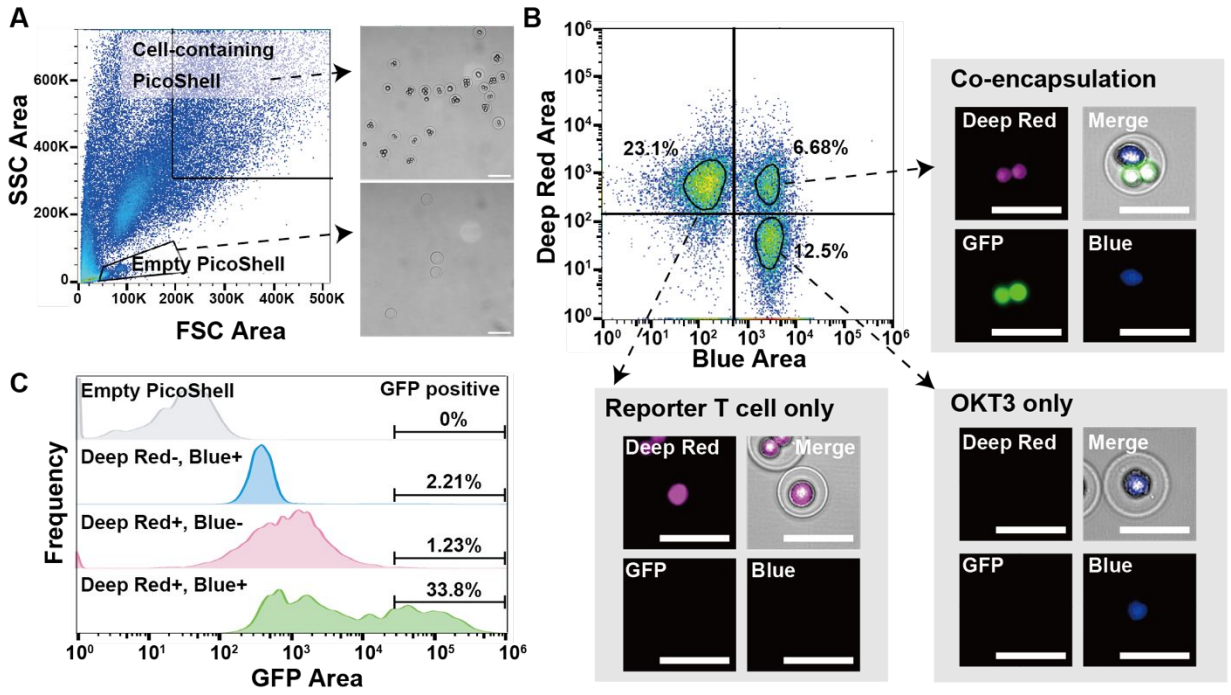

Figure 3. FACS analysis and sorting of reporter T cells co-encapsulated with OKT3. (A) Scatter plot showing empty and cell-containing PicoShells. Gated regions were sorted to identify regions with loaded vs. unloaded PicoShells. (B) Flow cytometry plot illustrating CellTracker Blue and CellTracker Deep Red intensities for PicoShells encapsulating cells, with the double-positive population representing co-encapsulated OKT3 and reporter T cells. Percentages of the total population within each gate are identified on the plot. Fluorescence microscopy, brightfield, and overlaid images of events sorted from each gate are shown. (C) Distribution of GFP intensity across empty events and PicoShells containing various combinations of cells. Percent of events within the high GFP gate are shown for each condition. Scale bars = 100 μm.

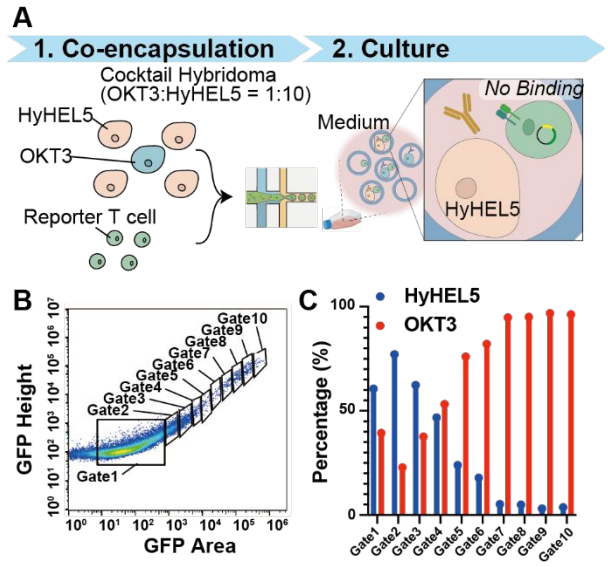

Figure 4. Selection of functional hybridomas activating reporter T Cells within PicoShells. (A) Schematic illustration of the spiked library workflow using a 1:10 ratio of OKT3 to HyHEL5 co-encapsulated with reporter T cells. (B) Gating strategy based on GFP levels to select hybridomas activating reporter T cells. (C) Purity of OKT3 and HyHEL5 cells across each selected gate, with cells identified using CellTracker Deep Red or Blue staining. Percentages indicate the proportion of blue- or deep red- positive cells within each gate.

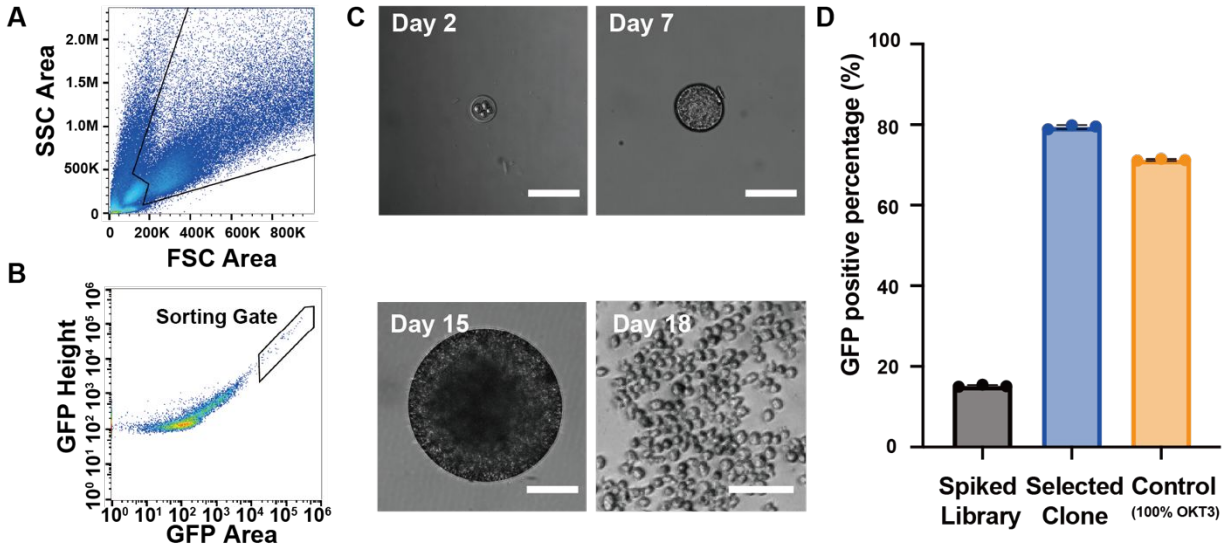

Figure 5. Spiked library screening with unlabeled 10% OKT3-spiked hybridoma library. (A) Cell sorting strategy selecting cell-containing PicoShells based on forward scatter area (FSC) and side scatter area (SSC). (B) PicoShells with the top 1% of GFP signal were sorted based on GFP Area. (C) Recovery of sorted hybridoma from PicoShells and cell expansion in growth medium over 18 days. (D) Functional validation of selected clones was performed by co-culturing the hybridoma clones with reporter T cells and measuring activation through GFP expression. Each dot represents a technical replicate, obtained by independently measuring the GFP expression levels for cells exposed to the same clone three times. Scale bars = 100 μm.

Author contributions

K.N. conceived and designed the study, performed the experiments, analyzed the data, developed new methods, prepared the figures, wrote the manuscript, and revised the manuscript. R.G. contributed to the study design and manuscript revision. M.v.Z. contributed to the conception and design of the study. D.F. performed the experiments. Z.M. and M.N. contributed to the study design. D.D.C. contributed to study conception, supervised the project, revised the manuscript, and acquired funding. All authors discussed the results and approved the final version of the manuscript.

Acknowledgement

This work was supported by JSPS Research Fellowship for Young Scientists (22KJ0996), JSPS Overseas Challenge Program for Young Researchers (202380180) and NSF grant # 2337423. We thank Owen N. Witte (University of California, Los Angeles) for generously sharing the reporter T cell line and Richard C. Willson (University of Houston) for generously sharing the HyHEL-5 hybridoma line. We are also

grateful to Shoji Takeuchi (The University of Tokyo) for his invaluable support and for providing the opportunity to conduct this collaborative research.

References

1 S. Jin, Y. Sun, X. Liang, X. Gu, J. Ning, Y. Xu, S. Chen and L. Pan, *Signal Transduct. Target. Ther.*, 2022, **7**, 39.
2 Z. Fu, H. Liu, L. Wang, C. Yu, Y. Yang, M. Feng and J. Wang, *Acta Pharm. Sin. B.*, 2021, **11**, 3925–3934.
3 Z. Chen, R. K. Kankala, Z. Yang, W. Li, S. Xie, H. Li, A.-Z. Chen and L. Zou, *Theranostics*, 2022, **12**, 3719–3746.
4 K. Shah, A. Al-Haidari, J. Sun and J. U. Kazi, *Signal Transduct. Target. Ther.*, 2021, **6**, 412.
5 J.-R. Hwang, Y. Byeon, D. Kim and S.-G. Park, *Exp. Mol. Med.*, 2020, **52**, 750–761.
6 J. E. Smith-Garvin, G. A. Koretzky and M. S. Jordan, *Annu. Rev. Immunol.*, 2009, **27**, 591–619.
7 N. Sandström, V. Carannante, K. Olofsson, P. A. Sandoz, E. L. Moussaud-Lamodière, B. Seashore-Ludlow, H. Van Ooijen, Q. Verron, T. Frisk, M. Takai, M. Wiklund, P. Östling and B. Önfelt, *Cell Rep. Methods*, 2022, **2**, 100256.
8 R. Vincken and A. Ruiz-Saenz, *STAR Protoc.*, 2023, **4**, 102224.
9 K. Le, C. Tan, H. Le, J. Tat, E. Zasadzinska, J. Diep, R. Zastrow, C. Chen and J. Stevens, *Biotechnol. J.*, 2020, **15**, e1900247.
10 B. El Debs, R. Utharala, I. V. Balyasnikova, A. D. Griffiths and C. A. Merten, *Proc. Natl. Acad. Sci. U. S. A.*, 2012, **109**, 11570–11575.
11 L. Mazutis, J. Gilbert, W. L. Ung, D. A. Weitz, A. D. Griffiths and J. A. Heyman, *Nat. Protoc.*, 2013, **8**, 870–891.
12 N. Shembekar, H. Hu, D. Eustace and C. A. Merten, *Cell Rep.*, 2018, **22**, 2206–2215.
13 Y. Wang, R. Jin, B. Shen, N. Li, H. Zhou, W. Wang, Y. Zhao, M. Huang, P. Fang, S. Wang, P. Mary, R. Wang, P. Ma, R. Li, Y. Tian, Y. Cao, F. Li, L. Schweizer and H. Zhang, *Sci Adv*, , DOI:10.1126/sciadv.abe3839.
14 A. Isozaki, Y. Nakagawa, M. H. Loo, Y. Shibata, N. Tanaka, D. L. Setyaningrum, J.-W. Park, Y. Shirasaki, H. Mikami, D. Huang, H. Tsoi, C. T. Riche, T. Ota, H. Miwa, Y. Kanda, T. Ito, K. Yamada, O. Iwata, K. Suzuki, S. Ohnuki, Y. Ohya, Y. Kato, T. Hasunuma, S. Matsusaka, M. Yamagishi, M. Yazawa, S. Uemura, K. Nagasawa, H. Watarai, D. Di Carlo and K. Goda, *Sci. Adv.*, 2020, **6**, eaba6712.
15 Y. Nakagawa, S. Ohnuki, N. Kondo, K. Itto-Nakama, F. Ghanegolmohammadi, A. Isozaki, Y. Ohya and K. Goda, *Lab Chip*, 2021, **21**, 3793–3803.
16 T. Beneyton, I. P. M. Wijaya, P. Postros, M. Najah, P. Leblond, A. Couvent, E. Mayot, A. D. Griffiths and A. Drevelle, *Sci. Rep.*, 2016, **6**, 27223.
17 A. Sciambi and A. R. Abate, *Lab Chip*, 2015, **15**, 47–51.
18 K. Fischer, A. Lulla, T. Y. So, P. Pereyra-Gerber, M. I. J. Raybould, T. N. Kohler, J. C. Yam-Puc, T. S. Kaminski, R. Hughes, G. L. Pyeatt, F. Leiss-Maier, P. Brear, N. J. Matheson, C. M. Deane, M. Hyvönen, J. E. D. Thaventhiran and F. Hollfelder, *Nat. Biotechnol.*, 2024, 1–11.
19 J. C. Weaver, P. McGrath and S. Adams, *Nat. Med.*, 1997, **3**, 583–585.
20 M. van Zee, J. de Rutte, R. Rumyan, C. Williamson, T. Burnes, R. Radakovits, A. Sonico Eugenio, S. Badih, S. Lee, D.-H. Lee, M. Archang and D. Di Carlo, *Proc. Natl. Acad. Sci. U. S. A.*, , DOI:10.1073/pnas.2109430119.
21 P. Kung, G. Goldstein, E. L. Reinherz and S. F. Schlossman, *Science*, 1979, **206**, 347–349.
22 P. A. Nesterenko, J. McLaughlin, B. L. Tsai, G. Burton Sojo, D. Cheng, D. Zhao, Z. Mao, N. J. Bangayan, M. B. Obusan, Y. Su, R. H. Ng, W. Chour, J. Xie, Y.-R. Li, D. Lee, M. Noguchi, C. Carmona, J. W. Phillips, J. T. Kim, L. Yang, J. R. Heath, P. C. Boutros and O. N. Witte, *Cell Rep.*, 2021, **37**, 110167.
23 T. Tang, H. Zhao, S. Shen, L. Yang and C. T. Lim, *Microsyst Nanoeng*, 2024, **10**, 3.

24 X. Luo and A. P. Lee, *Microfluid. Nanofluidics*, 2023, **27**, 1–12.
25 D. Di Carlo, D. Irimia, R. G. Tompkins and M. Toner, *Proc. Natl. Acad. Sci. U. S. A.*, 2007, **104**, 18892–18897.
26 J. F. Edd, D. Di Carlo, K. J. Humphry, S. Köster, D. Irimia, D. A. Weitz and M. Toner, *Lab Chip*, 2008, **8**, 1262–1264.
27 Z. Yao, C. T. J. van Velthoven, M. Kunst, M. Zhang, D. McMillen, C. Lee, W. Jung, J. Goldy, A. Abdelhak, M. Aitken, K. Baker, P. Baker, E. Barkan, D. Bertagnolli, A. Bhandiwad, C. Bielstein, P. Bishwakarma, J. Campos, D. Carey, T. Casper, A. B. Chakka, R. Chakrabarty, S. Chavan, M. Chen, M. Clark, J. Close, K. Crichton, S. Daniel, P. DiValentin, T. Dolbeare, L. Ellingwood, E. Fiabane, T. Fliss, J. Gee, J. Gerstenberger, A. Glandon, J. Gloe, J. Gould, J. Gray, N. Guilford, J. Guzman, D. Hirschstein, W. Ho, M. Hooper, M. Huang, M. Hupp, K. Jin, M. Kroll, K. Lathia, A. Leon, S. Li, B. Long, Z. Madigan, J. Malloy, J. Malone, Z. Maltzer, N. Martin, R. McCue, R. McGinty, N. Mei, J. Melchor, E. Meyerdierks, T. Mollenkopf, S. Moonsman, T. N. Nguyen, S. Otto, T. Pham, C. Rimorin, A. Ruiz, R. Sanchez, L. Sawyer, N. Shapovalova, N. Shepard, C. Slaughterbeck, J. Sulc, M. Tieu, A. Torkelson, H. Tung, N. Valera Cuevas, S. Vance, K. Wadhwani, K. Ward, B. Levi, C. Farrell, R. Young, B. Staats, M.-Q. M. Wang, C. L. Thompson, S. Mufti, C. M. Pagan, L. Kruse, N. Dee, S. M. Sunkin, L. Esposito, M. J. Hawrylycz, J. Waters, L. Ng, K. Smith, B. Tasic, X. Zhuang and H. Zeng, *Nature*, 2023, **624**, 317–332.
28 D. Challa, J. de Rutte, C. Konu, S. Udani, J. Liang, P. J. Krohl, R. Rondon, K. Bondensgaard, D. Di Carlo and J. Watkins-Yoon, *bioRxivorg*, 2024, 2024.08.15.608174.
29 J. de Rutte, R. Dimatteo, M. M. Archang, M. van Zee, D. Koo, S. Lee, A. C. Sharrow, P. J. Krohl, M. Mellody, S. Zhu, J. V. Eichenbaum, M. Kizerwetter, S. Udani, K. Ha, R. C. Willson, A. L. Bertozzi, J. B. Spangler, R. Damoiseaux and D. Di Carlo, *ACS Nano*, 2022, **16**, 7242–7257.
30 J. Langerman, S. Baghdasarian, R. Y.-H. Cheng, R. G. James, K. Plath and D. Di Carlo, *Nat. Protoc.*, , DOI:10.1038/s41596-024-01112-w.

Data Availability Statement

The data supporting this article have been included as part of the Supplementary Information. Raw data and .FCS files generated and analyzed during the current study are available from the corresponding author upon reasonable request.